

## Coherent Transfer of Spin through a Semiconductor Heterointerface

I. Malajovich, J. M. Kikkawa, and D. D. Awschalom

*Department of Physics, University of California, Santa Barbara, California 93106*

J. J. Berry and N. Samarth

*Department of Physics, Pennsylvania State University, University Park, Pennsylvania 16802*

(Received 8 September 1999)

Spin transport between two semiconductors of widely different band gaps is time resolved by two-color pump-probe optical spectroscopy. Electron spin coherence is created in a GaAs substrate and subsequently appears in an adjacent ZnSe epilayer at temperatures ranging from 5 to 300 K. The data show that spin information can be protected by transport to regions of low spin decoherence, and regional boundaries used to control the resulting spin coherent phase.

PACS numbers: 78.47.+p, 03.67.-a, 75.40.Gb, 75.70.Cn

A critical issue in the development of both magneto-electronic [1] and spin coherent [2] solid-state devices is the transmission of classical and quantum spin information through heterogeneous systems. The use of an electrical bias to draw polarized spins from a ferromagnet has succeeded in spin-resolving metallic and superconducting densities of state via tunneling [3], and has revealed giant magnetoresistance in metals containing ferromagnetic domains [4]. Although semiconductors provide additional control over spin lifetimes through doping [5], spin injection from ferromagnets into semiconductors has proved challenging [6] and has prompted all-optical investigations of spin transport in semiconductors [7,8]. Coherent spin transport has thus been seen in homogeneous crystals over macroscopic distances [8], and an extension of these phenomena to variable doping and band structure profiles creates additional opportunities for spin manipulation. Here we present an approach to interlayer spin transfer in which optical pulses excite and dynamically measure electron spin as it moves between GaAs and ZnSe semiconductors at temperatures from 5–300 K. Despite changes in doping and a twofold *increase* in band gap, the GaAs/ZnSe interface is not only surprisingly permeable to electron spin precession, but also modifies its amplitude and phase through associated discontinuities in the electron  $g$  factor.

Samples are Cl-doped ( $n \sim 5 \times 10^{17} \text{ cm}^{-3}$ ) 3000 Å ZnSe epilayers grown by molecular beam epitaxy on both semi-insulating (SI) and Si doped ( $n \sim 3 \times 10^{16} \text{ cm}^{-3}$ ) GaAs (100) substrates. Since the conduction band offset at ZnSe/GaAs heterojunctions ( $\sim 250\text{--}750 \text{ meV}$ ) is highly sensitive to interface conditions [9], we refrain from speculation about the detailed band alignment [Figs. 1(a)–1(b)]. In these pump-probe optical experiments [Fig. 1(c)], a circularly polarized pump pulse  $P$  creates electron spins oriented along the sample normal,  $\hat{x}$ .  $P$  may be tuned to either the ZnSe or GaAs absorption threshold (2.80 and 1.52 eV, respectively, at 5 K), and is denoted  $P_{ZS}$  or  $P_{GA}$ , accordingly. Whereas primary absorption of  $P_{ZS}$  occurs in ZnSe [Fig. 1(a)],  $P_{GA}$  passes through the ZnSe epilayer, exciting spins in the GaAs substrate [Fig. 1(b)]. The sub-

sequent Kerr rotation,  $\theta_K$ , of a linearly polarized probe pulse records the dynamics of the normal component of the total ZnSe spin,  $S_x(\Delta t)$  [Fig. 1(c)] [5]. Here,  $\Delta t$  is the pump-probe temporal interval and the probe's layer selectivity is obtained by tuning its energy within the range 2.70–2.80 eV to obtain maximum Kerr effect from the ZnSe epilayer at each temperature. The probe and  $P_{ZS}$  are split from the 100 fs output of a frequency-doubled, mode-locked Ti:sapphire laser and focused to a  $\sim 80 \mu\text{m}$  diameter spot.  $P_{GA}$  emerges from an additional Ti:sapphire cavity and focuses to  $\sim 20 \mu\text{m}$ . Whereas  $\Delta t$  is set using a conventional delay stage for  $P_{ZS}$ , for  $P_{GA}$   $\Delta t$  is set with 3 ps resolution by actively synchronizing pulse trains from both Ti:sapphire lasers [5]. Average power densities are 750 and 5  $\text{W cm}^{-2}$  for  $P_{GA}$  and  $P_{ZS}$ , respectively.

Figure 1(d) shows low-temperature, time-resolved Kerr rotation (TRKR) measurements of spin accumulation in ZnSe originating from  $P_{GA}$ . Data are shown at  $B = 0 \text{ T}$  as the pump energy  $E_P$  is tuned through the GaAs absorption threshold. In contrast to data obtained using  $P_{ZS}$ , in which signal appears suddenly at  $\Delta t = 0$  and then decays exponentially (not shown),  $P_{GA}$  produces a ZnSe magnetization  $S_x$  that grows over the first few hundred picoseconds and then decays with a spin lifetime appropriate to the ZnSe host. This suggests spin migration from GaAs to ZnSe, a suspicion confirmed by the sudden growth of  $S_x$  as  $E_P$  is tuned from below to above the GaAs absorption threshold [Fig. 1(e)]. The absence of signal below this threshold precludes a contribution from two-photon absorption in ZnSe. Conversely, the probe's selectivity in measuring only ZnSe spins is seen in Fig. 1(f), where  $\theta_K$  (and hence  $S_x$ ) is maximized at the ZnSe absorption threshold. An estimate of the fraction of GaAs spins entering ZnSe is 2.5%–10% at  $B = 0 \text{ T}$ , based on the Kerr response obtained by introducing a known number of spins directly into the ZnSe.

To estimate the spin arrival distribution, we extrapolate the exponential decay of the transferred spins back into the time of their arrival. This is shown in Fig. 2(a), where the dashed line fits the exponential decay from 2000 to 9000 ps and the shaded region marks the discrepancy

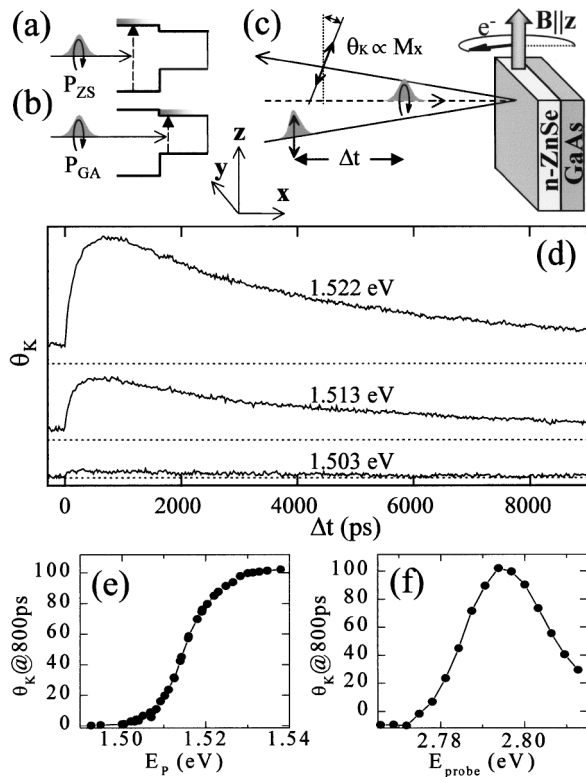


FIG. 1. (a),(b) Conduction and valence band diagram of a ZnSe(left)/GaAs(right) heterostructure. The conduction band offset is merely schematic and will generally include band bending and interface potentials. Excitation of spins in either ZnSe (a) or GaAs (b) is achieved by tuning the pump energy  $E_p$  to the appropriate interband absorption energy. (c) TRKR experimental geometry described in the text. The pump-probe noncollinear angle of  $3^\circ$  is exaggerated for clarity. (d) TRKR data for spin excitation in the SI GaAs substrate at  $T = 5$  K and  $B = 0$  T. The dashed lines mark  $\theta_K = 0$ . (e) Pump energy dependence of  $\theta_K$  at a fixed delay  $\Delta t = 800$  ps using a probe energy of  $2.80$  eV. (f) Probe energy dependence of  $\theta_K$  at  $\Delta t = 800$  ps and  $E_p = 1.52$  eV.

between this fit and the measured spin profile. Figure 2(b) shows this difference on a log scale for both substrates, where the data are normalized by the extrapolated spin amplitude and equal the fraction of spins yet to cross the interface. The data are well described by  $e^{-\Delta t/\tau}$ , where  $\tau$  is the accumulation time of spin transfer and equals  $210$  and  $440$  ps for SI and  $n$ -GaAs substrates, respectively. Generally,  $\tau = [\tau_0^{-1} + (T_2^*)^{-1}|_{\text{GaAs}}]^{-1}$ , where  $\tau_0$  is the spin accumulation time for nondecaying GaAs spins and  $T_2^*|_{\text{GaAs}}$  is the substrate transverse spin lifetime. The observed decrease in  $\tau$  for insulating substrates may then arise from a drop in  $T_2^*|_{\text{GaAs}}$  relative to the doped substrate [5], or from a doping dependence of band alignment, band bending, and spin diffusion. Presently, the relative contributions of electron transport and pure spin diffusion are unknown. Since the spin lifetime in the  $n$ -GaAs substrate is nearly 3 orders of magnitude longer than  $\tau$ , it appears that thermal relaxation may act to extinguish either process after a few hundred picoseconds. This might occur

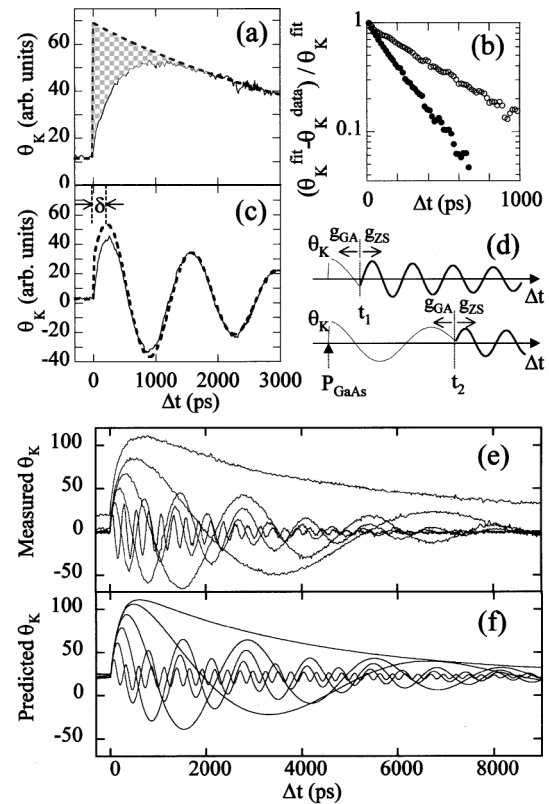


FIG. 2. (a) TRKR at  $B = 0$  T (solid line) for spins excited in an  $n$ -GaAs substrate. The dashed line shows the fit described within the text. The decay of the shaded amplitude (fit - data) gives a measure of the spin accumulation time in ZnSe. (b) A plot of the fraction of spins yet to cross into ZnSe. Both SI (solid circles) and  $n$ -doped (open circles) substrates are shown, with  $\tau = 210$  and  $440$  ps, respectively. (c) Data are similar to (a) but with  $B = 50$  mT. The temporal phase shift,  $\delta$ , is indicated. (d) Diagram showing spin dephasing arising from a difference between  $g_{\text{GA}}$  and  $g_{\text{ZS}}$ . Spin motion is simulated for ( $g_{\text{GA}} < 0, g_{\text{ZS}} > 0$ ) and two different arrival times in the ZnSe layer at  $\Delta t = t_1$  and  $t_2$ . (e) TRKR measured for  $B = 0, 10, 25, 50, 100,$  and  $250$  mT on a SI substrate. (f) TRKR predictions based on the  $B = 0$  T data using Eq. (2) and nominal  $g$ -factors for GaAs and ZnSe. All data taken at  $T = 5$  K and  $E_p = 1.522$  eV.

by reducing the carrier energy in GaAs below an interface potential or by moving spins into low energy states with reduced diffusion coefficients. And while the laser bandwidth  $\sim 13$  meV provides some initial kinetic energy, one might expect additional contributions from band bending at the interface. Interestingly, no significant changes in  $\tau$  are observed as  $E_p$  is increased to as much as  $40$  meV above the GaAs band edge.

The application of a transverse magnetic field  $B$  [Fig. 1(c)] induces coherent spin precession at the Larmor frequency,  $\omega = g\mu_B B/\hbar$  [5]. As discussed elsewhere,  $T_2^*$  places a lower bound on the rate of extra-electronic spin decoherence in the system [5]. Figure 2(c) shows the evolution of  $S_x$  at  $50$  mT, where spin precession results in an oscillatory profile,

$S_x(\Delta t \gg \tau) = Ae^{-\Delta t/T_2^*} \cos(\omega \Delta t + \phi)$ . For  $\Delta t \gg \tau$ , the data due to  $P_{GA}$  resembles that obtained from  $P_{ZS}$  (not shown). As with the data at  $B = 0$  T, we extrapolate this “post-transfer” behavior to earlier  $\Delta t$  [dashed line in Fig. 2(c)], and the difference between this extrapolation and the measured data shows a nonzero accumulation time. Significantly, values of  $\omega$  and  $T_2^*$  determined from the post-transfer fit reflect the  $g$  factor and spin lifetime of the ZnSe layer.

Conventional inhomogeneous effects manifest as a dephasing of the spin system and a field-dependent suppression of  $T_2^*$ . Spin evolution is particularly inhomogeneous during spin transfer because GaAs and ZnSe have different  $g$ -factors ( $g_{GA}$  and  $g_{ZS}$ , respectively). Hence, we expect significant spin dephasing phenomena to occur only during spin accumulation. A field dependence of  $S_x$  is shown in Fig. 2(e) for the SI substrate, demonstrating a marked decrease in the coherent spin transfer amplitude,  $A$ , with increasing applied field. Moreover, as seen in Fig. 2(c), there is a significant temporal phase shift  $\delta \equiv -\phi/\omega$  of the spin precession. Neither of these effects is seen in studies exciting and measuring spin in the same layer [5]. A qualitative account of each can be obtained by considering inhomogeneous effects arising from differences between  $g_{GA}$  and  $g_{ZS}$ . In Fig. 2(c),  $\phi < 0$ , indicating that the angle of transferred spins is retarded compared to that of spins directly excited within ZnSe ( $\phi \approx 0$ ). This phase shift shows that the  $g$  factor prior to spin transfer is lower than afterwards. As illustrated in Fig. 2(d), when  $g_{GA} \neq g_{ZS}$ , the phase of electron spins in ZnSe depends on their duration in GaAs. Hence, a distribution of arrival times [Fig. 2(b)] can result in inhomogeneous dephasing within the population of transferred electron spins. Assuming that the Larmor angle in each material grows as  $\omega \Delta t$ , where  $\omega$  is now material dependent, the contribution at  $\Delta t$  of all the spins that have spent a time  $t_i$  in the GaAs is

$$s_i(\Delta t) = s(t_i)e^{-\Delta t/T_2^*} \cos[\omega_{GA}t_i + \omega_{ZS}(\Delta t - t_i)], \quad (1)$$

where  $s(t_i) \equiv (S/\tau)e^{-t_i/\tau}$  is the spin accumulation rate at  $\Delta t = t_i$  and  $S$  is the total spin transferred. Integration of (1) over  $t_i < \Delta t$  yields the total spin contribution

$$S_x(\Delta t) = Ae^{-\Delta t/T_2^*} [\cos(\omega_{ZS}\Delta t + \phi) - e^{-\Delta t/\tau} \cos(\omega_{GA}\Delta t + \phi)], \quad (2)$$

where  $\phi = \tan^{-1}[\tau(\omega_{GA} - \omega_{ZS})]$ . During spin accumulation, the dephasing process phase shifts the spin precession and suppresses the spin amplitude,  $A \equiv S[1 + (\tan\phi)^2]^{-1/2}$ , as the applied magnetic field increases. In contrast to spin dephasing due to local field fluctuations or  $g$ -factor dispersion, this inhomogeneous process ceases once spin accumulation in the ZnSe is complete ( $\Delta t \gg \tau$ ).

Here we attempt to use the functional form for  $S_x(\Delta t)$  to extrapolate spin behavior from 0 T to nonzero fields. A fit to the 0 T data in Fig. 2(e) determines the zero-field values of  $S$ ,  $\tau$ , and  $T_2^*$ . Using nominal values of  $g_{GA} =$

$-0.44$  and  $g_{ZS} = 1.1$ , determined from spin precession measurements on these systems [5], Eq. (2) then predicts how  $S_x(\Delta t)$  might evolve as the field increases (assuming that  $A$ ,  $\tau$ , and  $T_2^*$  are field independent). These theoretical plots [Fig. 2(f)] exhibit many qualitative similarities with the actual data [Fig. 2(e)], including a decrease in the spin amplitude and a negative phase shift of spin precession.

Nonetheless, quantitative discrepancies remain, such as a field dependence of the ZnSe transverse spin lifetime that was held constant in Fig. 2(f). Figure 3(a) shows  $T_2^*$  versus  $B$  for both SI and  $n$ -GaAs substrates, obtained by fitting the spin decay from 2000–9000 ps, where  $\Delta t \gg \tau$  so that the second term in Eq. (2) vanishes. The decrease in  $T_2^*$  with field mirrors changes in  $T_2^*$  obtained by pumping spins directly into the ZnSe layer (also shown), and appears to describe properties of the

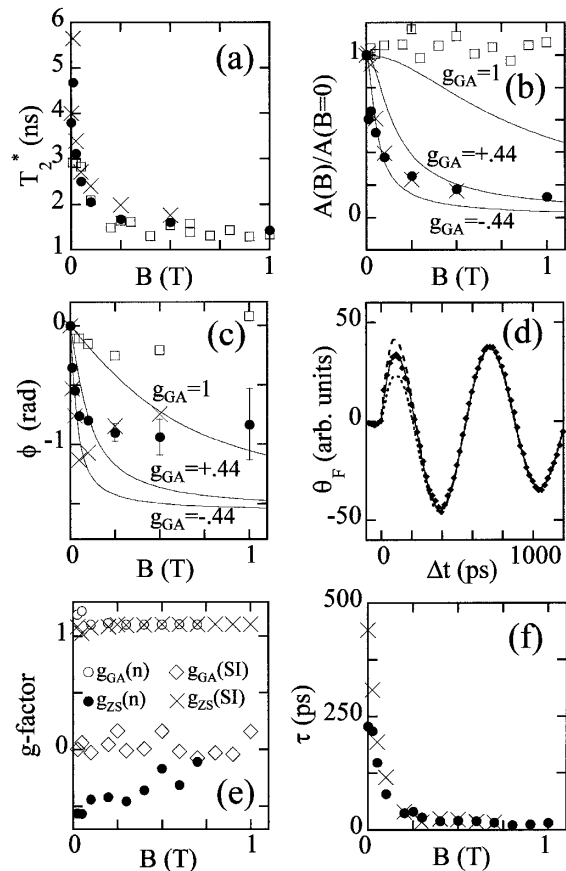


FIG. 3. (a)  $T_2^*$  vs  $B$  for excitation in the ZnSe layer (open squares), SI GaAs substrate (solid circles), and  $n$ -GaAs substrate (crosses). (b) Magnetic field dependence of the spin amplitude, normalized by its value at 0 T, and (c) phase shift. Legends in (b) and (c) are as in (a), and solid lines are contours of Eq. (2) at fixed values of  $g_{GA}$  with other parameters determined at zero field. (d) Sensitivity of fits over the entire time interval at 100 mT to  $g_{GA}$  [ $+0.04$  (solid line),  $+0.44$  (dotted line), and  $-0.44$  (dashed line)]. The first 1.2 ns is shown to emphasize discrepancies. The fitting procedure described in the text is used to determine (e)  $g_{GA}$  and  $g_{ZS}$ , and (f) the field dependence of the spin accumulation time for  $n$ -GaAs and SI GaAs substrates. All data taken at  $T = 5$  K and  $E_P = 1.522$  eV.

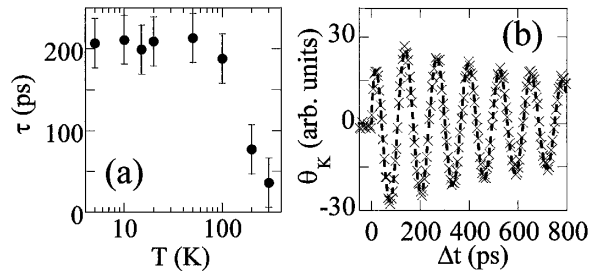


FIG. 4. (a) Temperature dependence of  $\tau$  at  $B = 0$  T. (b) TRKR measured (crosses) and fit (dashed line) at 300 K and  $B = 0.5$  T. All data taken on a SI substrate.

ZnSe host unrelated to the process of spin transfer. In contrast, the field-induced suppression of  $A$  and decrease in  $\phi$ , while similar for both substrates, occur despite a constancy of each obtained when spin excitation targets the ZnSe layer [Figs. 3(b)–3(c)]. The solid lines show predictions based on zero-field data, taking  $\Delta t \gg \tau$  as above. These contours of fixed  $g_{\text{GA}}$  show that no single field-independent value of  $g_{\text{GA}}$  is satisfactory. Using Eq. (2) to fit the data over the *entire* time interval, we find that  $g_{\text{GA}}$ ,  $A$ , and  $\tau$  must be taken as field dependent. In this case, Eq. (2) provides a five-parameter flexibility in fitting the data; however, four of these ( $g_{\text{ZS}}$ ,  $\phi$ ,  $T_2^*$ ,  $A$ ) may be determined from data at  $\Delta t \gg \tau$ . A subsequent fit over the full time interval then determines  $g_{\text{GA}}$  (and thereby  $\tau$ ). Figure 3(d) shows the sensitivity of this latter fit to  $g_{\text{GA}}$  (and hence  $\tau$ ), where it is seen that although  $g_{\text{GA}} = -0.44$  gives a fairly good match to the data, much better agreement is obtained for  $g_{\text{GA}} = 0.04$ . Figure 3(e) shows the  $g$  factors obtained by the full fitting procedure for both substrates. Note that while  $g_{\text{ZS}}$  is constant at 1.10,  $g_{\text{GA}}$  unexpectedly departs from its nominal value of  $-0.44$ . Since  $g_{\text{GA}}$  reflects only those GaAs spins that ultimately cross the interface, deviations may be due to excess kinetic energy within the incident spins, whose  $g$  factor is known to depend on wave vector [10] and can cross zero for carrier energies of 10–100 meV. Moreover, as seen in Fig. 3(f),  $\tau$  drops sharply with applied field, an effect that may arise from heretofore neglected effects of  $B$  on carrier kinetics such as cyclotron motion and band alignment. Since a similar decrease is seen in both substrates, for which  $T_2^*|_{\text{GaAs}}$  differs by nearly 3 orders of magnitude [5], it is clear that a field dependence of  $T_2^*|_{\text{GaAs}}$  alone cannot explain the observed behavior.

To gain further insight into the incident carrier kinetics, we study the temperature dependence of spin accumulation. Figure 4(a) shows that at  $B = 0$  T,  $\tau$  is roughly constant up to 100 K and decreases sharply thereafter. Once again, these changes may reflect a temperature dependence of the interface potential, the substrate spin lifetime, or perhaps an increase in the mean carrier velocity, but more extensive study is necessary to confirm these trends as  $\tau$  appears to vary with probe energy. As seen in Fig. 4(b), the transfer of spin induces coherence in ZnSe even at 300 K, where we observe no significant decrease in the measured signal. Equation (2) continues to describe the dynamics of the system at this temperature, as shown by the excellent agreement between data and fit.

Additional study is required to determine the relative contributions of charge and pure spin diffusion in these systems, to quantify the degree of spin decoherence occurring at the interface, and to discover if interface spin mobility is bidirectional. We thank ARO DAAG55-98-1-0366, DARPA/ONR N00014-99-1-1096 and N00014-99-1-1093, NSF DMR-9701072 and DMR-9701084, and ONR N00014-99-1-0077 and N00014-99-1-0071 for support.

- 
- [1] G. A. Prinz, *Science* **282**, 1660 (1998).
  - [2] D. P. DiVincenzo, *Science* **270**, 255 (1995).
  - [3] R. Meservey, P. M. Tedrow, and P. Fulde, *Phys. Rev. Lett.* **25**, 1270 (1970).
  - [4] S. S. P. Parkin, R. Bhadra, and K. P. Roche, *Phys. Rev. Lett.* **66**, 2152 (1991); J. Q. Xiao, J. S. Jiang, and C. L. Chien, *Phys. Rev. Lett.* **68**, 3749 (1992); A. E. Berkowitz, J. R. Mitchell, M. J. Carey, and A. P. Young, *Phys. Rev. Lett.* **68**, 3745 (1992).
  - [5] J. M. Kikkawa *et al.*, *Science* **277**, 1284 (1997); J. M. Kikkawa and D. D. Awschalom, *Phys. Rev. Lett.* **80**, 4313 (1998).
  - [6] F. G. Monzon and M. L. Roukes, *J. Magn. Magn. Mater.* **198**, 632 (1999), and references therein.
  - [7] D. Hagele, M. Oestreich, W. W. Ruhle, N. Nestle, and K. Ebert, *Appl. Phys. Lett.* **73**, 1580 (1998).
  - [8] J. M. Kikkawa and D. D. Awschalom, *Nature (London)* **397**, 139 (1999).
  - [9] V. Pellegrini *et al.*, *Appl. Phys. Lett.* **69**, 3233 (1996); J. B. Wang *et al.*, *Phys. Rev. B* **56**, 1416 (1997).
  - [10] M. J. Yang *et al.*, *Phys. Rev. B* **47**, 6807 (1993).